Utilizing Machine Learning to Identify Pigmented Lesion Types Using Images and Patient Metadata

Benjamin Joseph Lucero Herrera

High School Senior, BASIS Ahwatukee

ABSTRACT

With machine learning being being able to improve predictability and classification overtime, it has become possible to predict what was deemed unpredictable many decades ago. One such example is the classification of lesions via images or patient details. Now, there are multiple neural network models that can predict the lesion of a patient with a fairly satisfying degree of accuracy. However, many have only used image data rather than using both images and metadata. The goal of this research paper is to research whether or not the utilization of these two different data types can score higher accuracies, to understand if this method is viable, and to research the best model architecture to achieve this level of accuracy. This research paper will only go over the best model produced during this study and not discuss the details of other models.

1. Introduction

Ever since the first discovery of artificial intelligence (AI) and machine learning (ML) techniques, researchers have developed new approaches in making computers behave more like humans and become better than humans in different fields. Such advancements have led to improvements in regression modeling (Agarap 2019) to the creation of groundbreaking board game AIs like DeepBlue and AlphaGo (Campbell et al. 2002; Lapan 2018).

With recent discoveries happening constantly in the field of AI and ML, there have been major improvements in the sub-realm of image classification. The first image classification model was made in 1980 by Kunihiko Fukushima which constructed the idea of convolutional layers and downsampling layers (Fukushima 1980). This research would lead to the creation of convolutional neural network (CNN) which have become the standard neural network type for image classification and regression. Since then, new techniques were made to improve CNNs' accuracy. New discoveries include the concept of maxpooling (Yamaguchi 1990), 7-level convolution layer architecture in LeNet-5 (LeCun et al. 1998), and the VGG16 architecture (Simonyan and Zisserman 2015). Such advancements were further accelerated with the discovery of Graphics Processing Unit (GPU) implementation into ML models (Chellapilla et al. 2006). This implementation allowed ML models to train three times faster on GPUs compared to a standard Central Processing Units (CPU).

CNN techniques have been refined enough to be easily used in a wide variety of applications

while maintaining a relatively high standard of accuracy. One such application in which CNNs can be used is in the medical field where CNNs can be used for cancer identification via X-Ray imaging (Gordienko et al. 2019). One application that hasn't been fully researched yet is the identification of pigmented lesion types. There have been many studies in which CNNs were able to identify a specific type of lesions with a relatively decent accuracy. However, most of these researches failed to utilize both skin images and patient metadata to predict the type of lesions patients have.

The goal of this paper is to see if the utilization of the two types of data can help improve classification accuracy and to research the best possible concatenated CNN architecture that will input these types of data. It will be able to predict the correct pigmented lesion with a medium to high level degree of accuracy, while being able to generalize well with unprecedented data. The dataset used for this paper will come from the HAM10000 dataset (Tschandl 2018) which holds 10,015 images and rows of metadata. This dataset has seven different pigmented lesion classifications: Melanocytic Nevi (NV), Melanoma (MEL), Benign Keratosis-like Lesions (Solar Lentigines, Seborrheric Keratosis, and Lichenoid Keratosis; BKL), Basal Cell Carcinoma (BCC), Actinic Keratosis and Intraepithelial Carcinoma (AKIEC), Vasular skin lesions (VASC), and Dermatofibroma (DF). Architectures analyzed in this paper have drawn influence from past CNN architectures that have been proven to work well in image classification.

The paper proceeds as follows. Section 2 describes a brief background behind the seven types of lesion classification listed above. The materials used in this research and a dissection of the dataset are described in Section 3. The methodology used for this study is described in Section 4. Results are presented in Section 5. Analysis of this research study are discussed on Section 6. And a conclusion will be held on Section 7.

2. Background

a. *Melanocytic Nevi*

Also known as a mole, NV is a benign skin lesion that are composed of melanocytes that colonizes the epidermis. (Damsky and Bosenberg 2017). NV can be obtained via at birth or after birth. Respectively, these types of nevi are called congenital melanocytic naevus and acquired naevus (Marghoob 2002; Roh 2015). There are many other variants of NV such as Spitz Nevus, Reed Naevus, Agminated Naevi, and Kissing Naevus.

Melanocytes in NV are located similarly to melanocytes in the epidermis. The difference between normal and benign melanocytes is that benign melanocytes do not exhibit contact inhibition. This leads to a build-up of melanocytes which forms a nest which then forms a nevus. The exact reason for this exhibition is not well known. However, some factors that can influence this benign behavior can be ultraviolet (UV) exposure, genetic factors, and immune status. It has been noted that those with past family members with similar conditions can develop NV. (Ballone et al. 1999; English et al. 2006).

NV can be located on any part of the body and can even spread after blistering events and burns. Depending on the site of body, NV can differ in shape and size. NV can appear flat or round and can attain a pink, dark brown, blue, or black color. Individuals with lighter skin color tend to have lighter looking nevi while those with dark skin color tend to have darker nevi. Those with NV during their childhood tend to keep the nevi for life (Ródenas et al. 1996; Green et al. 1999; Autier et al. 2003).

b. *Melanoma*

MEL is similar to NV, but can be much more serious with life threating conditions. This is because malignant melanocytes inside MEL can penetrate through the dermis and travel to other parts of the body via blood vessels. This in return

leads to metastasis and the development of tumors in vital organs (Poole et al. 2005). However, most cases of MEL are benign and don't pose any threat to affected persons.

Similarly, the exact causes of MEL are unknown. However, one potential factor for the growth of MEL is UV exposure. It has been noted that UV radiation can cause immune suppression which can interfere with the immune system's cancer detection mechanics, allowing malignant melanocytes to travel throughout the body. (Kripke 1991). Others have pointed out that genetic factors can influence malignancy in metatocytes. In one observation. a heritable disease called Xeroderma pigmentosum helped develop non-melanomas skin cancer which has helped increase the risk of forming MEL in affected patients (Lynch et al. 1967). Though, a full understanding of how MEL can form has not been achieved yet due its complex nature.

The appearances and the location of MEL are similar to that of NV. MEL can have a tannish look to a darker black appearance and can appear similarly to NV. What differentiates MEL from NV is the changing of properties. If, the mole looks asymmetrical, has an irregular border, changes in color, is bigger than 6 mm, and is rapidly evolving over time, the skin lesion in question is most likely a MEL (Schadendorf et al. 2015).

c. *Benign Keratosis-like Lesions*[1]

Seborrheic Keratosis (SK) is a benign skin tumor where Keratinocytes in the epidermis proliferate much more than normal. This leads to a keratosis where it is cosmetically problematic and can be irritating. These skin lesions have a brown, black, or light tan color and can look waxy, scaly, and can be elevated. Common areas where SK can appear are on the head, neck, chest, and back. In terms of sizing, SK can reach up to 1 centimeter in diameter. SK tends to be prominent on elderly people (those 50 years old or older) and tend to increase in frequency in more older populations (Hafner and Vogt 2008). It is unknown how SK can formulate on an individual's skin. However, studies have shown linking UV exposure to the occurrences of SK (Yeatman 2008; Kwon 2003).

Solar Lentigines (SL) is a benign skin lesion where melanocytes proliferate more than normal, and a buildup of melanin occurs. This results in a darkened patch of skin which is diagnosed as SL. Unlike NV, MEL, or SK, SL has a definitive cause in which sun exposure causes the occurrence of SL (Bastiaens 2004). SL usually appears brown, but can range from a yellow-tan color to a brow-blacker color. Common areas where SL can arise are on the face, arms, dorsa of the hands, and upper part of the trunk. This type of skin lesion is common among indivduals with the ages of 30 to 50 years. SL is similar to severity to that of SK where is can be a cosmetic problem, but isn't irritating (Pollefliet et al. 2013).

Lichenoid Keratosis (LK) is another benign skin lesion where a small patch of skin is an inflamed macule or a pigmented plaque. LK is thought to be an inflammatory reaction to new epidermal growth. The exact cause for this inflammatory event is unknown (Morgan et al. 2005). However, it is possible that LK can develop where areas were affected by SK or SL (Elgart 2001). LK can appear from a reddish brown to a purplish brown color and can be big as 3 mm to 20 mm. LK can develop in persons ranging 30 to 80 years old and is more common in females than males (Goette 1980).

d. *Basal Cell Carcinoma*

BCC is a form of skin cancer where basal cells in the epidermis proliferate abnormally. If these basal cells penetrate through the epidermis, it is possible for these cells to spread and metastasize to other parts of the body. However, this is very rarely life-threatening (Wong et al. 2003). Individuals with past experiences with

[1] The background behind Seborrheic Keratosis, Solar Lentigines, and Lichenoid Keratosis are briefly described for this sub-section as examples for this class.

BCC have an increased risk of reocurrence, risk of developing other types of skin cancer, and other types of cancers that are beyond the scope of the skin. The most common forms of BCC are nodular, superficial, morphoeic, and basosquamous (Rubin et al. 2005).

BCC can be characterized as a brown, black, or blue lesion. These lesions can also have a pearl-white color or a pinkish-red hue. It can also be transparent in which blood vessels are visible if spectated at a close-enough distance. The physical shape of the cancer can be either flat or elevated. Sizes of BCC can range from a few millimeters to several centimeters in diameter. In terms of texture, it can be waxy, scaly, or scar-like. Areas that have been exposed to UV radiation can develop BCC and are commonly where BCC is located (Crowson 2006).

It is not yet clear to how BCC can develop in an individual's skin. However, some factors that increase a person's chance of developing BCC is constant exposure to the sun, immunosuppressive medication, arsenic exposure, radiation therapy, increasing age, and inheritance of genetics related to skin cancer (Telfer et al. 1999). BCC is more prominent to men than it is to women, with a male-to-female ratio of 2:1. Those above the age of 10 can develop BCC (Röwert-Huber et al. 2007).

e. *Actinic Keratosis and Intraepithelial Carcinoma*

Also known as Solar Keratosis, Actinic Keratosis (AK) is a precancer that forms on the skin of an affected individual. AK can form due to persistent exposure to UV light and many more can develop once the first AK is fully developed. If left untreated, the affected individual risks developing Squamous Cell Carcinoma which is much more life-threating (Figueras 2017).

AK can appear in a variety of colorations ranging from pink to brown. Physically, AK can be either flat or slightly elevated and can be up to 2.5 centimeters in diameter. The texture of this lesion can be rough, dry, hard, scaly, or water-like and can cause itching, burning, bleeding, or crusting (Jeffes and Tang 2000). The typical cause for AK is usually exposure to UV rays from the sun. The chances of an individual developing AK can increase if the individual is over 40 years old, exposes themselves frequently to UV radiation, or has a weakened immune system (Memon et al. 2001; Dodds et al. 2014).

Intraepithelial Carcinoma / Bowen's Disease (IC) is a precancer, similar to AK, that forms on the outermost layer of the skin. Similarly, IC can occur when an individual is exposed to UV radiation for too long and can be threating if left untreated. If IC is untreated, the lesion can turn into Squamous Cell Carcinoma, likewise to AK (Kao 1986).

IC has an appearance of a red or pink patch of skin that can look scaly or crusty. It either be flat or elevated if compared to surrounding skin. IC can resemble eczema, fungus, or psoriasis, and can often be mistaken for these skin conditions. This lesion can also cause irritation and bleeding of the nodule. Compared to AK, IC can be bigger in size as the skin lesion can grow up to 5 to 6 centimeters (Zalaudek et al. 2004). UV exposure is a common factor to the development of IC, but aging, weakened immune systems, and arsenic exposure play a potential role in the growth of IC (Cox et al. 2007).

f. *Vascular Skin Lesions*[2]

Known as red moles, Cherry Angiomas (CA) is a benign vascular skin lesion. The growth of CA is caused by irregular proliferation of endothelial cells. Unlike most other lesions that develop due to UV exposure, CA arises due to genetic factors of an individual. Though, the exact reason for the growth of CA is debatable (Klebanov et al. 2019).

[2] Vascular Skin Lesion is a broad category of skin lesions. Cherry Angioma and Angiokeratoma are briefly described in this sub-section as an example for this category.

CA attains a red, blue, or purple color and can range from 0.1 to 1 centimeter in diameter. These lesions can appear raised or flat. If the angioma is scratched, rubbed, or cut open, bleeding can occur. Common areas where CA can be located are torso, arms, legs, and shoulders (Natalie et al. 2020). Persons over the age of 40 years have a mediocre chance of developing CA and those over 75 years of age have a higher chance of developing it. However, adolescents can obtain this condition at a much lower risk (Tindall and Smith 1963).

Angiokeratoma (AGK) is another benign vascular skin lesion. This condition occurs when papillary dermis undergo hyperkeratosis or acanthosis. AGK has several different types: Angiokeratoma Corporis Diffusum, Angiokeratoma of Mibelli, Angiokeratoma of Fordyce, and Angiokeratoma Circumscriptu. Treatment is not harmless and doesn't mandate an immediate treatment. However, medical attention may be necessary if the development of AGK is from Fabry Disease (Grewal et al. 2018).

AGK can appear to be a red, blue, purple, or black papule with a rough, scaly, or thick surface. AGK can be recessed, flatten, or elevated compared to surrounding skin. This condition can be small as 1 millimeter to 5 millimeters. It can be mistaken for rashes, genital warts, or herpes. Other than Fabry Disease deriving from genetic reasons, AGK has no known reason for its development. AGK can affect all ranges of ages and both males and females (Ramsay et al. 1990; Imperial and Helwig 1967; Opitz et al. 1965).

g. *Dermatofibroma*

Dermatofibroma (DF) is a benign cutaneous fibrous histiocytoma. It is unclear how DF develops in the skin of an individual, but some studies have shown that it can be possible that DF is a neoplastic process where fibroblasts proliferate abnormally (Chen et al. 2000). It also has been noted that inflammatory and immunosuppression conditions may give way to the development of DF (Plaszczyca et al. 2014). DF is not life threatening as it cannot give rise towards cancer. DF is relatively common amongst any ages. Females tend to develop DF more frequently than males with a female-to-male ratio of 2:1 (Han et al. 2011).

DF usually size from 7 to 10 millimeters in diameter. However, the histiocytoma can grow up to 0.5 to 1.5 centimeters in diameter. It can grow anywhere on the skin, but is usually found on the skin of the lower legs. DF can appear red, purplish, gray, or brown and can be flat or protruded. DF doesn't cause symptoms to affected persons, but can be painful or itchy. It is often mistaken for Dermatofibrosarcoma Protuberans or Desmoplastic Melanoma (Zelger et al. 2004).

3. Materials

a. *Dataset and Dissection*

The dataset used for this research project will be the HAM10000 dataset which contains 10,015 images and rows of patient metadata. This dataset contains the following columns of data: lesion ID (lesion_id), image ID (image_id), pigmented lesion type (dx), confirmation type of lesion (dx_type), age, sex, and localization. Image ID and lesion ID are identification tags that helps locate which image is associated to which metadata. Pigmented lesion type identifies the image's lesion type from one of the seven classifications. The confirmation types for the image is how the lesion was confirmed. The four types of confirmation methods are histopathology, follow-up, expert consensus, and confirmation by in-vivo confocal microscopy. Localization pertains to where the image of the lesion was taken. Age and sex are self-explanatory.

b. *Training Hardware*

The training hardware for this research project proceeds as follows. The CPU used is a Ryzen 7 3800X at stock speeds (Base speed of 3.9GHz and Boost speed of 4.3Ghz). The GPU used for accelerated training is a RTX 2060 at a

base speed of 1680Mhz and 6GB of GDDR6 memory. The amount of RAM allocated for this project is 32 GB at 3200MHz.

c. *Software*

The software library utilized for machine learning is TensorFlow v2.3.1. Pandas v1.2.1, NumPy v1.18.5, and SciKit-Learn v0.0 are the libraries used for data manipulation, analysis, and preprocessing. Plots and graphs created for this study were created using TensorBoard v2.4.1 The programming language used for this project is Python v3.7.5 and virtual environment software used for package control is VirtualENV v3.7.5.

4. Methodology

The first step in this study is to clean and sort the data. Any row of data that fail to provide a value or is unknown must be omitted from the study. All values of dx_type will also be omitted from the study. It is reasonable to remove this type of data as they are identification methods used to diagnose the lesion a patient has. Another technique that may be used is to remove some rows of data that contain too much of the same lesion types. However, this step can be skipped if there is too little data to train on models. Once the data has been sorted, the next step is to normalize the images and metadata. For images, normalization can be achieved by divided each RGB value by 255. As for metadata, a MinMax Scaler normalization technique is used. The next step is to feed the data through several different types of models. Figure 1 shows a baseline model for this study. Results will be collected from loss graphs and accuracy graphs, and will be presented and discussed in later sections of this paper.

5. Results[3]

Model Ω follows the structure presented in Figure 1. However, Ω differs from the presented architecture as a batch normalization layer proceeds each layer excluding the metadata input layer and the softmax layer. Figure 2 shows the full architecture of model Ω.

There are three "branches" that makes up the model. The first branch is the image processing branch. This branch is responsible of passing image RGB values through multiple different convolutional, max pooling, and dropout layers. The second branch is the metadata branch. This branch simply inputs the three types of patient metadata: localization, sex, and age. The third branch is the fully connected branch which concatenates all of the outputs from the first and second batch and passes the data through a fully connected neural network. The model then outputs seven different results which represents the seven possible skin lesion types.

In the first branch, RGB values from images with a dimension of 200x150 are passed down through a series of convolutional, max pooling, and dropout layers. All layers in the model have a L2 weight regularizer of a hyperparameter value of 0.01. Convolutional layers in this model have a filter size of 2x2, 2D max pooling layers have a pooling size of 2x2, and all dropout layers have a dropout rate of 25%.

The third branch inputs the processed data from the first branch and the metadata from the second branch, and concatenates them together. They are then fed through ReLU layers with a dimension size of 1x1x4096 and dropout layers. After passing the data through the ReLU layers and dropout layers, the data is then passed to a SoftMax layer where it will present a prediction of whether the image and metadata presented is associated to one of the seven lesion types.

[3] The best model produced during this study will only be presented. This model will be referred to as "Model Ω" or "Ω." All other models made will be ignored.

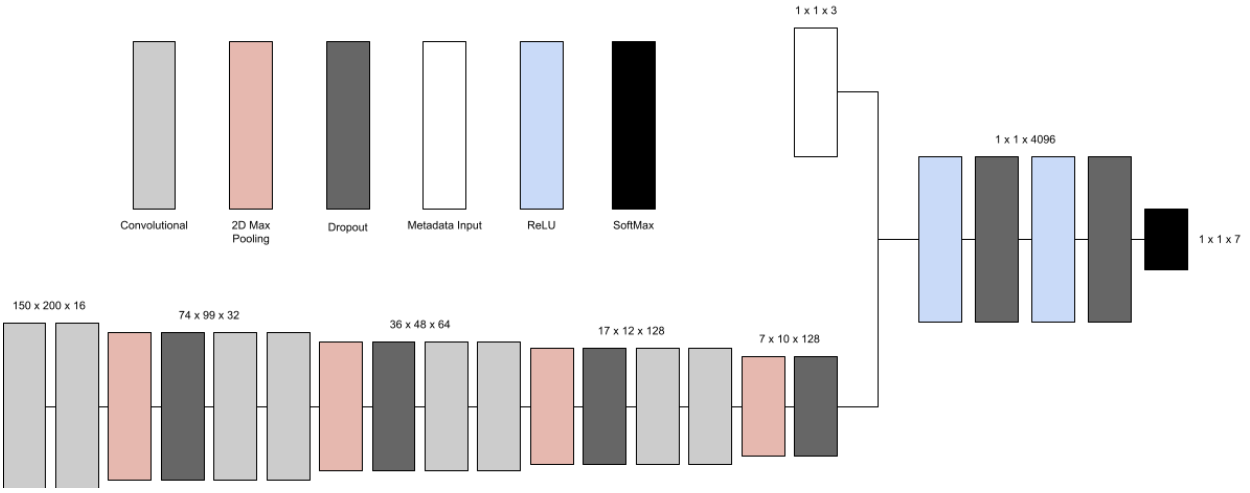

Figure 1: An example neural network architecture. Layer dimensions are presented for each group of layers.

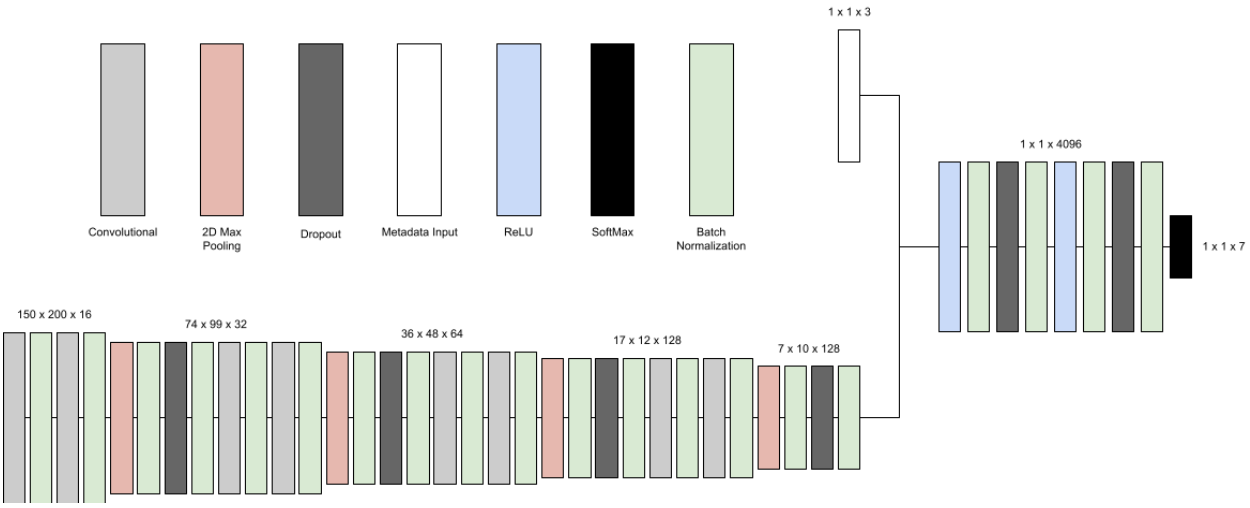

Figure 2: Architecture for Model Ω. Layer dimensions are presented for each group of layers.

The model was trained with the ADAM optimizer with a learning rate of 0.0001. The batch size for this model was 16, the number of epochs trained was 200 epochs, and the validation split percentage was 20%.

Ω produced satisfying results. From epochs 0 to 60, the validation loss decreases steadily until after epoch 60 where the validation loss started to increase noticeably. The training loss decreased slowly overtime. For accuracy, the validation accuracy decrease slowly as the model was trained on more epochs. Training accuracy exhibited a consistent rate of growth. The highest recorded accuracy of Model Ω (Measured by validation accuracy) was 83.05% with a training accuracy of 69.20%, validation loss of 4.356, and a training loss of 2.968. Figure 3 displays the losses and accuracies graphs for Model Ω.

6. Analysis

The accuracy graph demonstrates a high level of variance of accuracy during training. The accuracies reaches as low as 6.61% to 83.05%. This validation accuracy decreases overtime as the model is trained continuously. While validation accuracy diminishes overtime, the

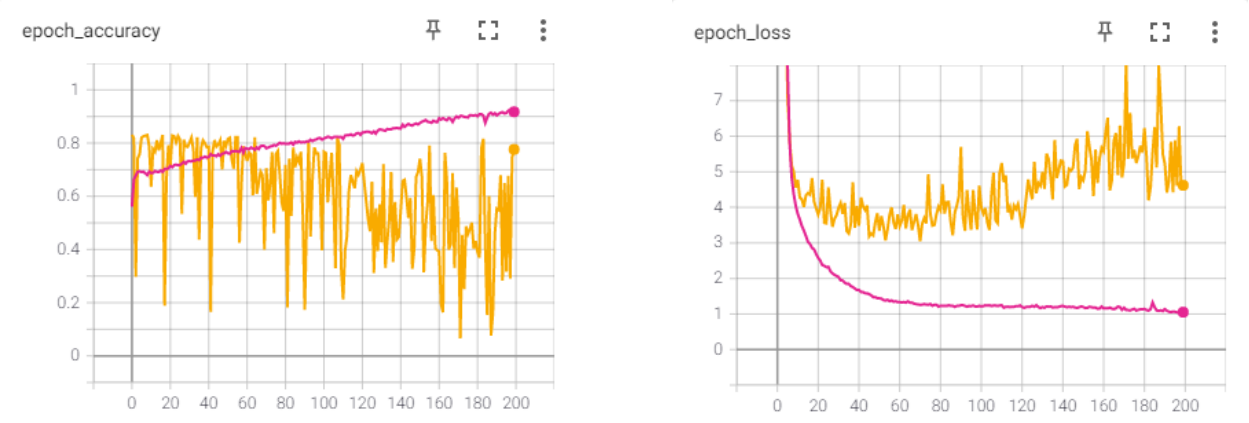

Figure 3: (Left) Accuracy graph of Model Ω. (Right) Loss graph of Model Ω. Yellow curves represent validation accuracy/loss and pink curves represent training accuracy/loss.

training accuracy increases at a steady rate.

In a broad view, the accuracy graph initially shows the training curve to be under the validation curve from epochs 0 to 65. The positioning of the two curves raises concerns of the model underfitting. This concern can be neglected as the training curve proceeds to grow above the validation curve and that from epochs 0 to 65, the loss curves of the model exhibited normal training behavior (validation and training loss curves decrease overtime).

During epochs 0 to around 65, we see the model trained normally as the validation and raining loss curves decreased. After around epoch 65, the validation began to increase in value, showing signs of overfitting.

7. Conclusion

With the use of a concatenated CNN, the results were satisfactory. The most accurate epoch with Model Ω is on epoch 16 with an accuracy of 83.05% and with a validation loss of 4.356. However, if the model were to be measured on a loss-sided approach, epoch 70 would be the best model with a validation loss of 3.048 and an accuracy of 78.06%.

With this level of accuracy, model Ω's architecture is a viable method of lesion classification (and possibly other disease classifications) that require an image of the affected area or disease and patient metadata. By increasing the size of the model and reducing the complexity of image preprocessing branch, it is possible to increase the classification accuracy.

Several techniques weren't utilized during this study due to technical issues and time constraints. Such examples are Bayesian Hyperparameter optimization and data augmentation. This model has the potential to produce higher degrees of accuracy. However, more work needs to be done as numerous aspects available for this research were not experimented, observed, or analyzed.

The source code for this project is available on GitHub for review[4].

REFERENCES

Agarap, Abien Fred M. "Deep Learning using Rectified Linear Units (ReLU)." 2019.

[4] Source code for this project is available at https://github.com/BenjaminHerrera/HAM10000-Research-Study

Autier, Philippe, et al. “Number and Size of Nevi Are Influenced by Different Sun Exposure Components: Implications for the Etiology of Cutaneous Melanoma (Belgium, Germany, France, Italy)” *Cancer Causes & Control,* vol. 14, no. 5, 2003, pp.453-459.

Ballone, Enzo, et al. “Pigmentary traits, nevi and skin phototypes in a youth population of Central Italy.” *European Journal of Epidemiology,* vol. 15, no. 2, 1999, pp.189-195.

Bastiaens, Maarten, et al. “Solar Lentigines are Strongly Related to Sun Exposure in Contrast to Ephelides.” *Pigment Cell Research,* vol. 17, no. 3, 2004, pp. 225-229.

Campbell, Murray, et. al. “Deep Blue.” *Artificial Intelligence,* vol. 134, 2002, pp. 57-83.

Chellapilla, Kumar, et al. “High Performance Convolutional Neural Networks for Document Processing.” *Tenth International Workshop on Frontiers in Handwriting Recognition,* 2006.

Cox, N., et al. “Guidelines for management of Bowen's disease: 2006 update.” *British Journal of Dermatology,* vol. 156, no. 1, 2007, pp. 11-21.

Crowson, A. “Basal cell carcinoma: biology, morphology and clinical implications” *Modern Pathology,* vol. 19, 2006, pp. 127-147.

Damsky, W E, and M Bosenberg. “Melanocytic nevi and melanoma: unraveling a complex relationship.” *Oncogene*, vol. 36, no. 42, 2017, pp. 5771-5792.

Dodds, Annabel, et al. “Actinic Keratosis: Rationale and Management.” *Dermatology and Therapy,* vol. 4, 2014, pp. 11-31.

Elgart, George W. “Seborrheic Keratoses, Solar lentigines, and Lichenoid Keratoses: Dermatoscopic Features and Correlation to Histology and Clinical Signs” *Dermatologic Clinics,* vol. 19, no. 2, 2001, pp. 347-357.

English, Dallas R., et al. “Ultraviolet Radiation at Places of Residence and the Development of Melanocytic Nevi in Children (Australia).” *Cancer Causes & Control,* vol. 17, no. 1, 2006, pp. 103-107.

Figueras, M. T. Fernandez. “From actinic keratosis to squamous cell carcinoma: pathophysiology revisited.” *Journal of the European Academy of Dermatology and Venereology,* vol. 31, 2017, pp. 5-7.

Fukushima, Kunihiko. “Neocognitron: A Self-organizing Neural Network Model for a Mechanism of Pattern Recognition Unaffected by Shift in Position.” *Biological Cybernetics,* vol. 36, 1980, pp. 193-202.

Goette, Detlef K. “Benign Lichenoid Keratosis.” *Archives of Dermatology,* vol. 116, no. 7, 1980.

Gordienko, Yu, et al. “Deep Learning with Lung Segmentation and Bone Shadow Exclusion Techniques for Chest X-Ray Analysis of Lung Cancer.” *ICCSEEA,* 2018.

Green, Adele, et al. “A Case-Control Study of Melanomas of the Soles and Palms (Australia and Scotland)” *Cancer Causes & Control*, vol. 10, no. 1, 1999, pp. 21-25.

Hafner, Christian and Vogt, Thomas. “Seborrheic Keratosis.” *Journal Der Deutschen Dermatologischen Gesellschaft,* vol. 6, no. 8, 2008, pp. 664-677.

Houghton, Alan N., and Polsky, David. "Focus on melanoma." *Cancer Cell*, vol. 2, no. 4, 2002, pp. 275-278.

Jeffes, Edward W. B., and Tang, Emily H. “Actinic Keratosis.” *American Journal of Clinical Dermatology,* 2000, pp. 167-179.

Kao, Grace F. “Carcinoma Arising in Bowen's Disease.” *Archives Dermatology,* vol. 122, no. 10, 1986, pp. 1124-1226.

Klebanov, Nikolai, et al. “Use of Targeted Next-Generation Sequencing to Identify Activating Hot Spot Mutations in Cherry Angiomas.” *JAMA Dermatology,* vol. 155, no. 2, 2019, pp. 211-215.

Kripke, Margaret L. “Immunological Effects of Ultraviolet Radiation.” *The Journal of Dermatology,* vol. 18, 1991, pp. 429-433.

Kwon, Oh S., et al. “Seborrheic keratosis in the Korean males: causative role of sunlight” *Photodermatology, Photoimmunology, & Photomedicine,* 2003.

Lapan, Maxim. “Deep Reinforcement Learning Hands-On: Apply modern RL methods, with deep Q-networks, value iteration, policy gradients, TRPO, AlphaGo Zero and more.” *Packt Publishing Ltd*, 2018.

LeCun, Yann, et al. “Gradient-Based Learning Applied to Document Recognition”. *Proc. Of the IEEE,* 1998.

Lynch, H. T., et al. “Xeroderma Pigmentosum, Malignant Melanoma, and Congenital Ichthyosis.” *Arch Dermatology,* vol. 96, no. 6, 1967, pp. 625-635.

Marghoob, Ashfaq A. “Congenital melanocytic nevi: Evaluation and management.”

Dermatologic Clinics, vol. 20, no. 4, 2002, pp. 607-616.

Memon, A., et al. "Prevalence of solar damage and actinic keratosis in a Merseyside population." *British Journal of Dermatology,* vol. 142, no. 6, 2001, pp. 1154-1159.

Morgan, M. B., et al. "Benign Lichenoid Keratosis A Clinical and Pathologic Reappraisal of 1040 Cases." *The American Journal of Dermatopathology,* vol. 27, no. 5, 2005, pp. 387-392.

Pollefliet, Caroline, et al. "Morphological characterization of solar lentigines by in vivo reflectance confocal microscopy: a longitudinal approach." *International Journal of Cosmetic Science,* vol. 35, no. 2, 2013, pp. 149-155.

Poole, Catherine M., et al. "Prevention, Detection, and Treatment." *Yale University Press,* 2005.

Ródenas, José M, et al. "Sun Exposure, Pigmentary Traits, and Risk of Cutaneous Malignant Melanoma: A Case-Control Study in a Mediterranean Population" *Cancer Causes & Control,* vol. 7, no. 2, 1996, pp. 275-283.

Roh, Mi Ryung, et al. "Genetics of melanocytic nevi." *Pigment Cell Melanoma Res,* vol. 28, 2015, pp. 661-672.

Röwert-Huber, J., et al. "Epidemiology and aetiology of basal cell carcinoma." *British Journal of Dermatology,* vol. 157, 2007, pp. 47-51.

Rubin, Adam I, et al. "Basal-Cell Carcinoma" *New England Journal of Medicine,* vol. 353, no. 21, 2005, pp. 2262-2269.

Schadendorf, Dirk, et al. "Melanoma." *Nat Rev Dis Primers,* 2015.

Simonyan, Karen, and Zisserman, Andrew. "Very Deep Convolution Networks for Large-Scale Image Recognition." *ICLR,* 2015.

Telfer, N. R., et al. "Guidelines for the management of basal cell carcinoma" *British Journal of Dermatology,* vol. 141, 1999, pp. 415-423.

Tschandl, Philipp. "The HAM10000 dataset, a large collection of multi-source dermatoscopic images of common pigmented skin lesions." (V2). *Harvard Database,* 2018, https://doi.org/10.7910/DVN/DBW86T. Accessed 16 December 2020.

Wong, C. S. M, et al. "Basal cell carcinoma" *BMJ,* vol. 327, 2003, pp. 794-498.

Yamaguchi, Kouichi, et al. "A Neural Network for Speaker-Independent Isolated Word Recognition." *ICSLP,* vol. 90, 1990.

Yeatman, J. M., et al. "The prevalence of seborrheic keratoses in an Australian population: does exposure to sunlight play a part in their frequency?" *British Journal of Dermatology,* 2008.

Zalaudek, I., et al. "Dermoscopy of Bowen's disease." *British Journal of Dermatology,* vol. 150, no. 6, 2004, pp. 1112-1116.

Natalie, Buslach, et al. "Treatment Modalities for Cherry Angiomas: A Systematic Review." *Dermatologic Surgery,* vol. 46, no. 12, 2020, pp. 1691-1697.

Tindall, John, and Smith, J. "Skin Lesions of the Aged and Their Association with Internal Changes." *JAMA,* vol. 186, no. 12, 1963, pp. 1039-1042.

Grewal, A., et al. "A case report of adult-onset multiple angiokeratomas with zosteriform distribution." *Dermatology Online Journal,* vol. 24, no. 10, 2018.

Ramsay, Bart, et al. "Acral Pseudolymphomatous Angiokeratoma of Children." *Archives of Dermatology,* vol. 126, no. 11, 1990, pp. 1524-1525.

Imperial, Roland, and Helwig, Elson B. "Angiokeratoma of the Scrotum (Fordyce Type)" *The Journal of Urology,* vol. 98, no. 3, 1967, pp. 379-398.

Opitz, John M., et al. "The Genetics of Angiokeratoma Corporis Diffusum (Fabry's Disease) and Its Linkage Relations with the Xg Locus." *American Journal of Human Genetics,* vol. 17, no. 4, 1965, pp. 325-342.

Chen, Tse-Ching, et al. "Dermatofibroma is a clonal proliferative disease." *Journal of Cutaneous Pathology,* vol. 27, no. 1, 2000, pp. 36-39.

Plaszczyca, Anna, et al. "Fusions involving protein kinase C and membrane-associated proteins in benign fibrous histiocytoma." *The International Journal of Biochemistry & Cell Biology,* vol. 53, 2014, pp. 475-481.

Zelger, Bernhard, et al. "Dermatofibroma—A Critical Evaluation." *International Journal of Surgical Pathology,* vol. 12, no. 4, 2004, pp. 333-344.

Han, Tae Young, et al. "A clinical and histopathological study of 122 cases of dermatofibroma (benign fibrous histiocytoma)." *Ann Dermatology,* vol. 23, no. 2, 2011, pp. 185-192.